



Structure-based design and synthesis of macrocyclic peptidomimetic β -secretase (BACE-1) inhibitors

Rainer Machauer*, Siem Veenstra, Jean-Michel Rondeau, Marina Tintelnot-Blomley, Claudia Betschart, Ulf Neumann, Paolo Paganetti

Novartis Institutes for BioMedical Research, Novartis Pharma AG, PO Box, CH-4002 Basel, Switzerland

ARTICLE INFO

Article history:

Received 24 November 2008

Revised 9 January 2009

Accepted 14 January 2009

Available online 19 January 2009

Keywords:

Alzheimer's disease

BACE-1 inhibition

Macrocyclization

Hydroxyethylene transition-state mimetic

ABSTRACT

The hydroxyethylene octapeptide inhibitor OM99-2 served as starting point to create the tripeptide inhibitor **1** and its analogues **2a** and **b**. An X-ray co-crystal structure of **1** with BACE-1 allowed the design and syntheses of a series of macrocyclic analogues **3a–h** covalently linking the P1 and P3 side-chains. These inhibitors show improved enzymatic potency over their open-chain analogue. Inhibitor **3h** also shows activity in a cellular system.

© 2009 Elsevier Ltd. All rights reserved.

Alzheimer's disease (AD) is a devastating neuro-degenerative disorder characterized by progressive cognitive decline. At severe stages of the disease, AD patients cannot manage daily life and depend completely on caregivers. Since its description by Alois Alzheimer in 1907, the prevalence of AD is steadily increasing, mostly because of the growing aged population.¹ In spite of the rising demand for medication, no truly disease-modifying therapies are yet available. AD is characterized histopathologically by the occurrence of amyloid plaques and neurofibrillary tangles in the brain.² Three key findings underpin the current drug discovery efforts towards a therapy for AD: The detection of β -amyloid peptides ($\text{A}\beta_{40/42}$) as the main components of amyloid plaques,³ the identification of the amyloid precursor protein (APP),⁴ and the discovery of autosomal dominant mutations in the APP gene linked to early-onset AD.⁵ The β -amyloid hypothesis is now widely accepted as the central paradigm in the pathogenesis of AD.⁶ According to this model, aggregated β -amyloid peptides with 40 or 42 residues in length ($\text{A}\beta_{40/42}$) are neurotoxic and initiate a cascade of events leading to neuronal degeneration. $\text{A}\beta_{40/42}$ generation from APP requires two consecutive endoproteolytic cleavages. In a first step, APP is cleaved by BACE-1 (β -site APP cleaving enzyme), a membrane-bound aspartyl protease.⁷

The resulting membrane-tethered C99 fragment is further processed by γ -secretase releasing the neurotoxic $\text{A}\beta_{40}$ or $\text{A}\beta_{42}$. Since BACE-1 knock-out/APtransgenic mice are viable, but lack completely $\text{A}\beta_{40/42}$ and do not form amyloid plaques, BACE-1 inhibition

is widely considered an attractive therapeutic approach for the treatment and prevention of AD.⁸

Besides other hit finding activities, such as high throughput screening of large compound libraries using biochemical or binding assays, the sequence of the natural substrate protein is a classical starting point for a structure-based approach to protease inhibition. From past medicinal chemistry efforts to design inhibitors of renin and HIV protease, effective strategies to convert substrate-based peptidomimetics into drug-like inhibitors are well documented.⁹ However, endoproteases typically make use of several binding interactions along the substrate backbone within the active-site cleft to achieve low nanomolar binding affinities. This explains why their inhibitors often have a relatively high molecular weight (500 Da and above), triggering considerable subsequent efforts to optimize their pharmacokinetic properties. Large peptidomimetic inhibitors usually do not enter the brain due to their unfavorable physicochemical profile (high polar surface area and high number of H-bond donors and acceptors). While this is less of an issue for targets exclusively located in the periphery (e.g., renin), other indications require at least some degree of brain penetration (e.g., HIV protease). From this perspective, the structure-based design of a brain-penetrating BACE-1 inhibitor undoubtedly represents an extreme case and a formidable challenge. Having all the above mentioned issues in mind but confronted with a limited number of hits from high-through-put screenings we decided to test whether the substrate sequence can be reduced to a peptidic inhibitor of reasonable size and potency. If this proves feasible we thought further improvements of the pharmacokinetic and CNS penetration properties by reducing the number of rotatable

* Corresponding author. Tel.: +41 61 6963431; fax: +41 61 6962455.
E-mail address: rainer.machauer@novartis.com (R. Machauer).

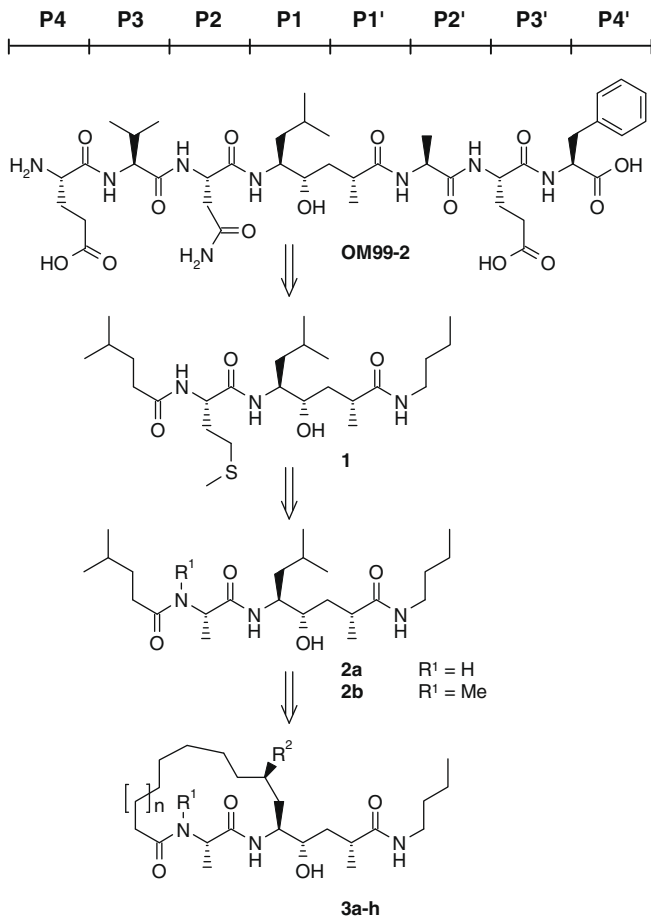


Figure 1. Peptide inhibitor OM99-2 and peptidic lead structures **1**, **2a/b** and macrocyclic inhibitors **3a–h** of BACE-1.

bonds,¹⁰ PSA, etc. should be possible as for HIV protease and could be addressed in next design cycles.

For our approach we started from OM99-2, using the first X-ray crystallography data of a ligand – BACE-1 complex published by Tang and collaborators.¹¹ This substrate-derived octapeptide inhibitor with nanomolar potency $K_i = 1.6 \text{ nM}$ (OM99-2, Fig. 1) is spanning the P4–P4' subsites. In order to define a minimal core of binding interactions, we first aimed at reducing the size of OM99-2 while preserving low micromolar activity. This effort resulted in compound **1**, a three residue hydroxyethylene transition-state inhibitor, exhibiting $1.4 \mu\text{M}$ potency in the BACE-1 enzymatic assay but only 12% inhibition at $10 \mu\text{M}$ in a cellular system.¹²

According to published subsite specificities for BACE-1, the methionine side-chain was not expected to contribute significantly to binding in S2.¹³ Its reduction to alanine was possible without major loss of activity, leading to compound **2a** with an activity of $3.7 \mu\text{M}$ in the enzymatic assay. Inspection of the X-ray structure of the OM99-2 – BACE-1 complex showed the absence of hydrogen bonded interactions between the P2/P3 amide nitrogen and the protein. We therefore prepared the *N*-methyl-alanine analogue **2b**. This more rigid open-chain inhibitor displayed enzymatic activity ($2.4 \mu\text{M}$) and cellular potency comparable to **1**.

The co-crystal structure of BACE-1 in complex with **1** was determined at 2.0 \AA resolution.¹⁴ The crystallographic data showed that the key binding interactions observed in the OM99-2 complex, in particular those involving the transition-state mimetic and the three backbone amide bonds, were conserved in the complex with inhibitor **1** (Fig. 2). The loss of binding energy resulting from the

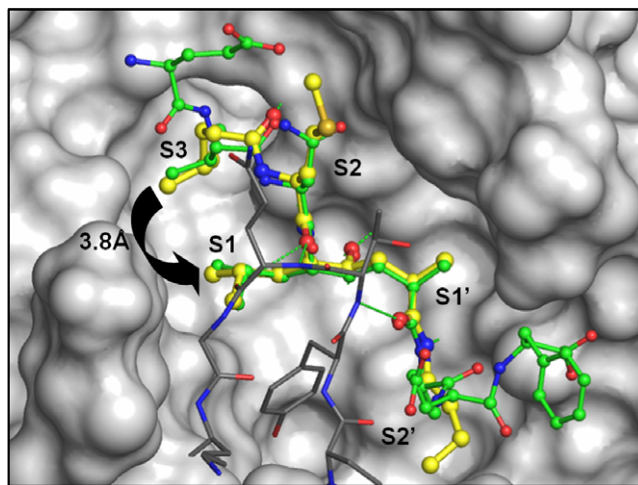


Figure 2. Cocrystal structure of **1** in complex with BACE-1. The BACE-1 active-site is shown in surface representation. For clarity the flap residues 69–75 (shown in gray sticks) were omitted from the surface calculation. **1** is shown in thick ball-and-stick with yellow carbon atoms. An overlay with OM99-2 is shown in thin ball-and-stick with green carbon atoms.

drastic reduction in size was partly compensated by more extensive hydrophobic interactions contributed by the C-terminal *n*-butylamino group in the S2' subsite, and by the N-terminal 4-methyl-pentanoic group occupying the S3 pocket. More importantly, the X-ray analysis showed that this amino-terminal alkyl group was in van der Waals contact (3.8 Å) to the P1 isobutyl group filling the neighboring S1 pocket, without any intervening enzyme residue. With the two alkyl side-chains in such close vicinity, the concept of bridging P1 and P3 was very appealing. Furthermore, the nearest protein residues (Leu30, Ile110, Trp115) were at a distance of about 4 Å, with the S1 and S3 subsites forming a continuous pocket lined by hydrophobic residues (Tyr71, Ile118, Phe108, Leu30, Trp115, Ile110). The topology of the BACE-1 active-site was thus found to be fully compatible with the introduction of a linker connecting P1 and P3.

The macrocyclization strategy was also supported by the success of this approach as an established method to pre-organize and stabilize bioactive conformations, especially tripeptide β -strands.¹⁵ Its effectiveness has already been demonstrated for other aspartic proteases, and we were hoping to earn at least some of its expected benefits in terms of improved enzymatic potency, cellular activity/permeability and proteolytic stability.¹⁶ During the course of our project other groups also published on related approaches for BACE-1 inhibitors.¹⁷

Molecular modeling – docking studies using QXP/mcdock in the Flo modeling package¹⁸ – indicated the use of a two- or three-carbon linker to connect the P1 and P3 side-chains. As suggested by the P1/P3 distance in the bound conformation of **1**, a 14-membered macrocycle was calculated to bring the P1 and P3 alkyl chains too close together thus resulting in suboptimal occupation of the S3 pocket. The 15-membered ring was predicted to improve S3 filling, but a solvent accessible surface representation showed that the fit was not yet optimal. Thus, enlarging the ring by one further carbon to a 16-membered ring appeared to preserve optimally the relaxed conformation of P1 and P3 while achieving the best fit with regard to Leu30 and Trp115. In contrast, the 17-membered ring was predicted to be too bulky for the pocket forcing the macrocycle into a conformation which would be energetically less favorable and clearly less tightly fitting. The model of the 15- or 16-membered macrocycles favored in QXP docking calculations are shown in Figure 3.

Furthermore, modeling suggested the conservation of the resulting methyl group in P1 with (R)-stereochemistry, while the

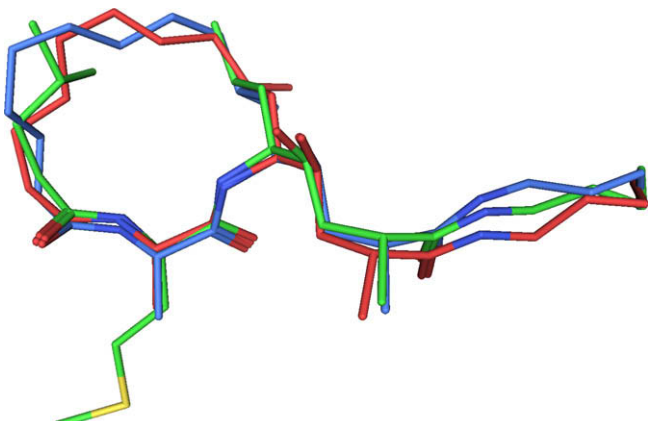


Figure 3. Examples for 15-membered (red) and 16-membered (blue) macrocycles as modeled in the X-ray structure of **1** (green).

resulting methyl group in P3 – in the model close to the Gln12/Gly13 amide – was deemed less crucial. In order to explore the validity of this approach, the macrocyclic analogues **3a–h** (Fig. 1) of compounds **2a** and **b** were synthesized.

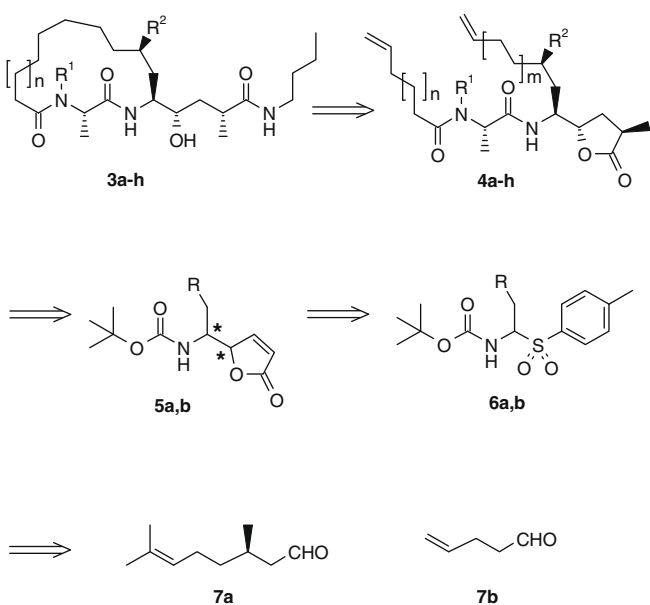
As outlined in Scheme 1 we prepared the macrocyclic inhibitors **3a–h** by ring-closing metathesis (RCM) followed by aminolysis of the δ -lactone and hydrogenation. The cyclization precursors **4a–h** were obtained from the dipeptide isostere precursors **5a** and **b** by hydrogenation of the internal double bond, diastereo-selective alkylation and standard coupling and deprotection steps, followed by separation of the two diastereomers. (In case of **5a** the triple substituted double bond was also converted into a terminal double bond.)

The unsaturated δ -lactones **5a** and **b** were synthesized by addition of lithiated 5H-furan-2-one into the corresponding amido-sulfones **6a** and **b**. We applied this approach since we had observed in preceding exploratory experiments that this addition gave selectively access to the two trans (threo) isomers of the four possible addition products (unpublished results). This reaction and its selectivity for which we did not find any literature precedence thus represent a new method for the synthesis of hydroxyethylene

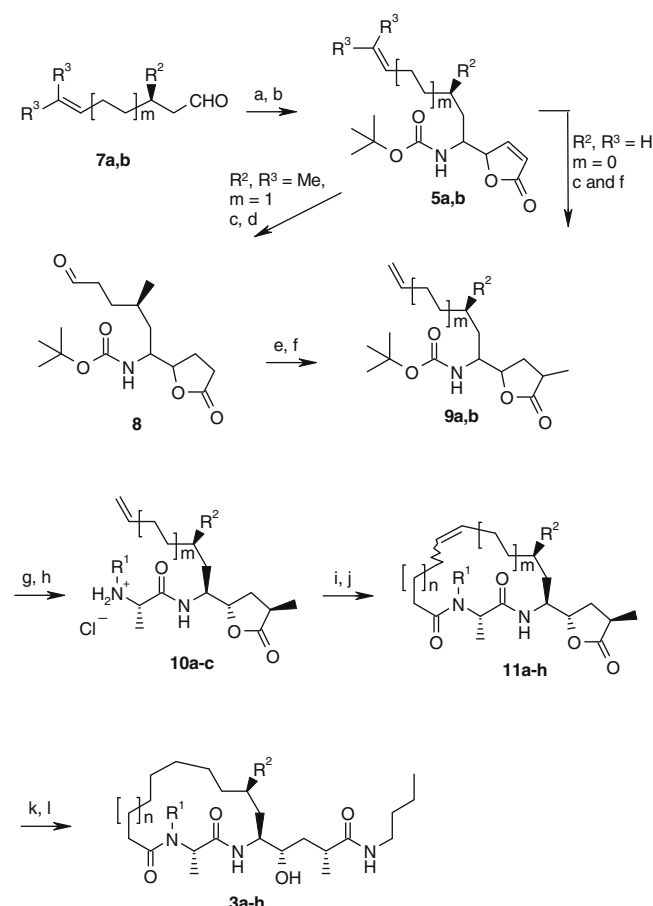
dipeptide isosteres. The acyl-imminium equivalents **6a** and **b** were accessible from (*R*)-citronellal (**7a**) and pent-4-enal (**7b**) by a standard condensation procedure.¹⁹

To prepare the macrocyclic inhibitors **3a–h** we started with the condensation of the aldehydes **7a** and **b** with sodium toluenesulfinate and *tert*-butyl-oxy carbonyl amine in the presence of formic acid, followed by the alkylation of the sulfinates with lithiated 2,5-dihydro-2-furanone (Scheme 2). The diastereomeric mixture of (*R*)-citronellal derived (*R,R*)- and (*S,S*)-butenolide **5a** was subjected to hydrogenation and ozonolysis to provide aldehyde **8**. Wittig reaction and alkylation afforded a diastereomeric mixture of lactone **9a**. The conversion of the triple substituted double bond into a terminal double bond was necessary since metathesis reactions with the triple substituted double bond were not successful. In case of the achiral aldehyde **7b** the butenolide **5b** was hydrogenated and methylated to provide **9b**. After amine deprotection and coupling with Boc-alanine or Boc-*N*-methyl-alanine the two diastereomers were separated by chromatography. Subsequent cleavage of the Boc group provided the central intermediates **10a–c**.

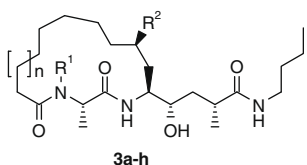
Various acids were coupled and ring-closing metatheses with Grubbs second generation catalyst afforded the macrocyclic olefins **11a–h**.²⁰ Opening of the δ -lactones with *n*-butylamine followed by hydrogenation provided the inhibitors **3a–h**.



Scheme 1. Retrosynthetic analysis of compounds **3a–h**.



Scheme 2. Reagents and conditions: (a) Sodium toluenesulfinate, BocNH_2 , formic acid; (b) 5H-furan-2-one, LHMDS, -70°C to -50°C , 81% for two steps; (c) H_2 , Raney-Ni; (d) ozone, PPh_3 , 92% for two steps; (e) $\text{Ph}_3\text{PCH}_2\text{Br}^-$, KOTBu , -40°C ; (f) LHMDS, DMPU, MeI, -78°C , 69% for two steps; (g) 4N HCl in dioxane; (h) Boc-AA-OH , HOEt, EDC, Et_3N , 74% for two steps, separation of 2 diastereomers; (i) 4N HCl in dioxane, 99%; alkenyl acid, HOEt, EDC, Et_3N ; (j) Grubbs 2nd generation catalyst, 40°C , 75% for two steps; (k) *n*-butylamine, 50°C ; (l) H_2 , Pd-C , 99% for two steps.

Table 1Enzymatic and cellular inhibition assay results for compounds **1**, **2a** and **b** and **3a–h**

Compound	R ¹	R ²	n	BACE-1 inhibition IC ₅₀ , μM ^a	Cellular inhibition % at 10 μM ^a	hCathD inhibition IC ₅₀ , μM ^a
1	H	–	–	1.4	12	0.37
2a	H	–	–	3.7	7 [*]	31% at 10 μM
2b	Me	–	–	2.4	10 [*]	34% at 10 μM
3a	H	Me	0	1.6 [*]	n.a.	n.a.
3b	H	Me	1	0.59	16 [*]	46% at 10 μM
3c	H	H	1	7.6	8 [*]	18% at 10 μM
3d	H	Me	2	0.25	27 [*]	1.7
3e	H	H	2	46% at 10 μM ^{**}	n.a.	n.a.
3f	H	Me	3	2.1 [*]	15 ^{**}	n.a.
3g	Me	Me	1	2.5	17 [*]	16% at 10 μM
3h	Me	Me	2	0.15	60	8.1

IC₅₀ values for BACE-1 and cathepsin D inhibition, and inhibition of cellular release of A_β40 were determined as described.¹²^a Values are means of at least three experiments (n.a., not available).^{*} Two measurements.^{**} Single measurement.

The binding data for the macrocycles **3a–h** were in good agreement with the predictions. The 14-membered macrocycle **3a** showed an activity of 1.6 μM in the enzymatic assay, which is only a 2-fold increase in activity over **2a** (Table 1). Expanding the macrocyclic core by one methylene unit to the 15-membered ring **3b**, did indeed increase the activity to 0.59 μM. The 6-fold improvement over compound **2a** was ascribed to a better stabilization of the bioactive conformation. But the increase in potency in the enzymatic assay was only partly reflected in the cellular activity (16% reduction of A_β_{1–40} release at 10 μM), which was only improved 2-fold over the matching open-chain analogue **2a**.

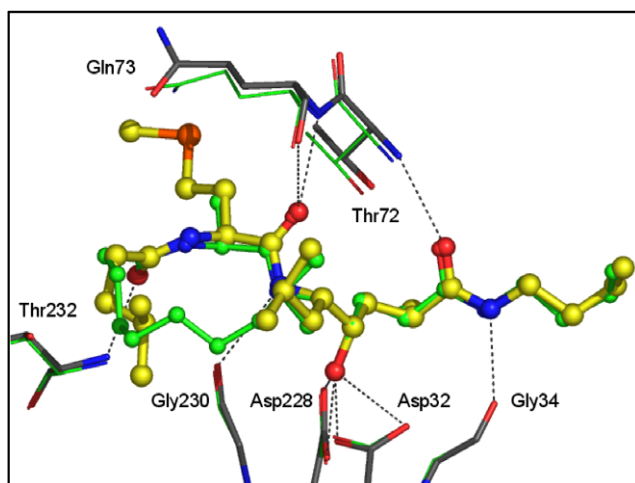
Crystallographic analysis at 2.1 Å resolution of the BACE-1 complex with **3b** fully confirmed the modeling predictions regarding the binding mode of the inhibitor, and the conformation of active-site residues (Figure 4).

As shown in Figure 4, the cyclization had hardly any effect on the binding of the P1 and P2 groups, while the position of the hydroxyethylene transition-state mimic and the P' groups were not affected at all by this modification. The alkyl linker was in-

volved in hydrophobic contacts to Leu30 (3.5 Å), Ile110 (3.8 Å) and Trp115 (4.0 Å). These interactions appeared to stabilize a different conformer of the Ile110 side-chain.

In line with the prediction, further ring-expansion to the 16-membered macrocycle **3d** proved to be optimal resulting in a potency of 0.25 μM in the enzymatic assay corresponding to a 15-fold improvement over **2a**. The critical importance of the P1 methyl group is demonstrated by the inhibitors **3c** and **3e** which lack this group and show a significant loss in activity compared to **3b** and **3d**. The cellular potencies of the inhibitors **3b–h** were also lower in comparison to the enzymatic activities by more than one order of magnitude. The peptidic character of the inhibitors **3a–f** was suspected to be responsible for the discrepancy between the enzymatic and the cellular potency, since these compounds encompassed three amide bonds. To test this hypothesis we removed the H-bond donor by N-methylation of the P2–P3 amide which does not contribute to BACE binding leading to macrocycles **3g** and **h**. Again in line with modeling predictions for the 15-membered analogue **3g** a slightly (4-fold) reduced potency in the enzymatic assay compared to **3b** was observed. While in the case of the 16-membered ring the P2/3N-methylated macrocycle fitted tightly and weakly improved (2-fold) the enzymatic activity over **3d**, to 0.15 μM for **3h**. The removal of the H-bond donor of the P2–P3 amide in the macrocycles **3g** and **h**, involving the replacement of one water molecule present in the X-ray, had no significant negative impact on their potency, similar to the open-chain analogues **2a** and **b**, but seemed to influence the preferred ring size. However, methylation of the P2–P3 amide in **3g** and **h** did not improve the potency in the cellular assay to an extent as seen in the enzymatic assay. For the most potent macrocycle **3h** the cellular activity of 8.7 (±0.9) μM remained 1–2 orders of magnitude lower than that determined in the enzymatic assay.

In parallel to the BACE-1 activity we also monitored the inhibition of human cathepsin D (CathD), a related aspartyl protease involved in lysosomal protein degradation and cancer.²¹ The peptidic lead structure **1** was 4-fold selective over CathD. Macrocyclization, different ring-sizes, and N-methylation of the P2–P3 amide improved BACE-1 selectivity over CathD. Compound **3d** displayed 6-fold selectivity, whereas the selectivity over CathD increased to 56-fold for the most potent BACE-1 inhibitor **3h**.

**Figure 4.** Overlay, based on protein C_α atoms, of the BACE-1 complexes with inhibitors **1** (yellow/grayscale carbon atoms) and **3b** (green carbon atoms).

In summary, we report the structure-based design of novel P1–P3 linked macrocyclic BACE-1 inhibitors based on crystallographic data obtained for the open-chain compound **1**. In agreement with modeling studies, the 15- and 16-membered macrocycles **3b** and **3d** were more active compared to their open-chain analogues **2a** and **b**, without increasing their molecular weight. The binding mode of **3b** to BACE-1 was confirmed by crystallographic analysis. Sufficient occupancy of P1 by methyl substitution of the alkyl chain appeared necessary to reach submicromolar BACE-1 inhibition. The macrocyclization alone did not improve cellular potency. Notably, the reduction of the peptidic character of the macrocyclic inhibitors by methylation of the P2/3 amide retained the enzymatic activity but did not improve the cellular activity to the same level. The macrocyclic inhibitors proved also to be weakly to moderately selective over the related aspartyl protease CathD.

Acknowledgments

For the BACE complex with **3b**, X-ray data collection was performed at the Swiss Light Source, Paul Scherrer Institut, Villigen, Switzerland. We are grateful to the machine and beamline groups whose outstanding efforts have made this experiment possible.

We thank C. McCarthy for proofreading the manuscript.

Supplementary data

Supplementary data associated with this article can be found, in the online version, at doi:10.1016/j.bmcl.2009.01.036.

References and notes

- (a) Alzheimer, A. *Alig. Z. Psychiat.* **1907**, 64, 146; (b) Alzheimer, A. *Cbl. Nervenheil. Psychiat.* **1907**, 30, 177; (c) Alzheimer, A. *Z. Neurol. Psychiat.* **1911**, 4, 356.
- Nussbaum, R. L.; Ellis, C. E. N. *Eng. J. Med.* **2003**, 348, 1356.
- Glenner, G. G.; Wong, C. W. *Biochem. Biophys. Res. Comm.* **1984**, 120, 885.
- Kang, J.; Lemaire, H. G.; Unterbeck, A.; Salbaum, J. M.; Masters, C. L.; Grzeschick, K. H.; Multhaup, G.; Beyreuther, K.; Müller-Hill, B. *Nature* **1987**, 325, 733.
- Van Broeckhoven, C.; Haan, J.; Bakker, E.; Hardy, J.; Van Hul, W.; Webnert, A.; Vegter-van der Vlis, M.; Roos, A. *Science* **1990**, 248, 1120.
- Hardy, J.; Selkoe, D. J. *Science* **2002**, 297, 353.
- (a) Vassar, R.; Bennett, B. D.; Babu-Khan, S.; Kahn, S.; Mendiaz, E. A.; Denis, P.; Teplow, D. B.; Ross, S.; Amarante, P.; Loeloff, R.; Luo, Y.; Fisher, S.; Fuller, J.; Edenson, S.; Lile, J.; Jarosinski, M. A.; Biere, A. L.; Curran, E.; Burgess, T.; Louis, J.-C.; Collins, F.; Treanor, J.; Rogers, G.; Citron, M. *Science* **1999**, 286, 735; (b) Yan, R.; Bienkowski, M. J.; Shuck, M. E.; Miao, H.; Tory, M. C.; Pauley, A. M.; Brashler, J. R.; Stratman, N. C.; Mathews, W. R.; Buhl, A. E.; Carter, D. B.; Tomasselli, A. G.; Parodi, L. A.; Heinrikson, R. L.; Gurney, M. E. *Nature* **1999**, 402, 533; (c) Sinha, S.; Anderson, J. P.; Barbour, R.; Basi, G. S.; Caccavello, R.; Davis, D.; Doan, M.; Dovey, H. F.; Frigon, N.; Hong, J.; Jacobson-Croak, K.; Jewett, N.; Keim, P.; Knops, J.; Lieberburg, I.; Power, M.; Tan, H.; Tatsuno, G.; Tung, J.; Schenk, D.; Seubert, P.; Suomensaari, S. M.; Wang, S.; Walker, D.; Zhao, J.; McConlogue, L.; John, V. *Nature* **1999**, 402, 537; (d) Hussain, I.; Powell, D.; Howlett, D. R.; Tew, D. G.; Meek, T. D.; Chapman, C.; Gloger, I. S.; Murphy, K. E.; Southan, C. D.; Ryan, D. M.; Smith, T. S.; Simmons, D. L.; Walsh, F. S.; Dingwall, C.; Christie, G. *Mol. Cell. Neurosci.* **1999**, 14, 419; (e) Lin, X.; Koelsch, G.; Wu, S.; Downs, D.; Dashti, A.; Tang, J. *Proc. Natl. Acad. Sci. USA* **2000**, 97, 1456.
- Luo, Y.; Bolon, B.; Kahn, S.; Bennett, B. D.; Babu-Khan, S.; Denis, P.; Fan, W.; Kha, H.; Zhang, J.; Gong, Y.; Martin, L.; Louis, J.-C.; Yan, Q.; Richards, W. G.; Citron, M.; Vassar, R. *Nat. Neurosci.* **2001**, 4, 231.
- (a) Rahuel, J.; Rasetti, V.; Maibaum, J.; Rueege, H.; Göschke, R.; Cohen, N. C.; Stutz, S.; Cumin, F.; Fuhrer, W.; Wood, J. M.; Grüter, M. G. *Chem. Biol.* **2000**, 7, 493; (b) Wood, J. M.; Maibaum, J.; Rahuel, J.; Grüter, M. G.; Cohen, N. C.; Rasetti, V.; Rueege, H.; Göschke, R.; Stutz, S.; Fuhrer, W. *Biochem. Biophys. Res. Commun.* **2003**, 308, 698; (c) Tomasselli, A. G.; Heinrikson, R. L. *Biochim. Biophys. Acta (BBA) – Protein Struct. Mol. Enzymol.* **2000**, 1477(1–2), 189.
- Veber, D. F.; Johnson, S. R.; Cheng, H.-Y.; Smith, B. R.; Ward, K. W.; Kopple, K. D. *J. Med. Chem.* **2002**, 45, 2615.
- (a) Hong, L.; Koelsch, G.; Lin, X.; Wu, S.; Terzyan, S.; Gosh, A. K.; Zhang, X. C.; Tang, J. *Science* **2000**, 290, 150; (b) Ghosh, A. K.; Bilcer, G.; Harwood, C.; Kawahama, R.; Shin, D.; Hussain, K. A.; Hong, L.; Loy, J. A.; Nguyen, C.; Koelsch, G.; Ermoloeff, J.; Tang, J. *J. Med. Chem.* **2001**, 44, 2865.
- (a) Hanesian, S.; Yun, H.; Hou, Y.; Yang, G.; Bayrakdarian, M.; Therrien, E.; Moitessier, N.; Roggo, S.; Veenstra, S.; Tintelnot-Blomley, M.; Rondeau, J.-M.; Ostermeier, C.; Strauss, A.; Ramage, P.; Paganetti, P.; Neumann, U.; Betschart, C. *J. Med. Chem.* **2005**, 48, 5175; (b) The cellular activity was determined in Chinese Hamster Ovary cells, stably transfected with human wild-type APP. Compounds (0.003–10 μ M) were incubated with adherent cells in 96 well plates ($n = 3$ for each concentration) for 24 h. Supernatant concentration of amyloid peptide 1–40 was analyzed using Europium-labeled beta-1 (N-terminus) and XL-665 labeled 25H10 (C-terminus) in-house antibody and homogenous time resolved fluorescence detection on a PHERAstar instrument (BMG Labtech, Offenburg, Germany). Cell viability was determined using MTT staining.
- Turner, R. T., III; Koelsch, G.; Hong, L.; Castanheira, P.; Gosh, A.; Tang, J. *Biochemistry* **2001**, 40, 10001.
- X-ray coordinates for the complex of BACE with inhibitors **1** and **3b** have been deposited in the Protein Data Bank (<http://www.rcsb.org>), and can be accessed under PDB ID: 3DUY and 3DV1.
- Reid, R. C.; Kelso, M. J.; Scanlon, M. J.; Fairlie, D. P. *J. Am. Chem. Soc.* **2002**, 124, 5673.
- (a) Driggers, E. M.; Hale, S. P.; Lee, J.; Terrett, N. K. *Nature Rev. Drug Disc.* **2008**, 7, 608; (b) Tyndall, J. D. A.; Reid, R. C.; Tyssen, D. P.; Jardine, D. K.; Todd, B.; Passmore, M.; March, D. R.; Pattenden, L. K.; Bergman, D. A.; Alewood, D.; Hu, S.-H.; Alewood, P. F.; Birch, C. J.; Martin, J. L.; Fairlie, D. P. *J. Med. Chem.* **2000**, 43, 3495, 43.
- (a) Ghosh, A. K.; Devasamudram, T.; Hong, L.; DeZutter, C.; Xu, X.; Weerasena, V.; Koelsch, G.; Bilcer, G.; Tang, J. *Bioorg. Med. Chem. Lett.* **2005**, 15, 15; (b) Rojo, I.; Martin, J. A.; Broughton, H.; Timm, D.; Erickson, J.; Yang, H.-C.; McCarthy, J. R. *Bioorg. Med. Chem. Lett.* **2006**, 16, 191; (c) Stachel, S. J.; Coburn, C. A.; Sankaranarayanan, S.; Price, E. A.; Wu, G.; Crouthamel, M.; Pietrak, B. L.; Huang, Q.; Lineberger, S. R.; Espeseth, A. S.; Jin, L. *J. Med. Chem.* **2006**, 49, 6147; (d) Lindsley, S. R.; Moore, K. P.; Rajapakse, H. A.; Selnick, H. G.; Young, M. B.; Zhu, H.; Munshi, S.; Kuo, L.; McGaughey, G. B.; Colussi, D.; Crouthamel, M.-C.; Lai, M.-T.; Pietrak, B.; Price, E. A.; Sankaranarayanan, S.; Simon, A. J.; Seabrook, G. R.; Hazuda, D. J.; Pudvah, N. T.; Hochman, J. H.; Graham, S. L.; Vacca, J. P.; Nantermet, P. G. *Bioorg. Med. Chem. Lett.* **2007**, 17, 4057; (e) Moore, K. P.; Zhu, H.; Rajapakse, H. A.; McGaughey, G. B.; Colussi, D.; Price, E. A.; Sankaranarayanan, S.; Simon, A. J.; Pudvah, N. T.; Hochman, J. H.; Allison, T.; Munshi, S. K.; Graham, S. L.; Vacca, J. P.; Nantermet, P. G. *Bioorg. Med. Chem. Lett.* **2007**, 17, 5831; (f) Barazza, A.; Götz, M.; Cadamuro, S. A.; Goettig, P.; Willem, M.; Steuber, H.; Kohler, T.; Jestel, A.; Reinemer, P.; Renner, C.; Bode, W.; Mororder, L. *ChemBioChem* **2007**, 8, 2078.
- McMartin, C.; Bohacek, R. S. *J. Comp. Aid. Mol. Des.* **1997**, 11, 333.
- Palomo, C.; Oiarbide, M.; Landa, A.; Gonzalez-Rego, M. C.; Garcia, J. M.; Gonzalez, A.; Odriozola, J. M.; Martin-Pastor, M.; Linden, A. *J. Am. Chem. Soc.* **2002**, 124, 8637.
- Scholl, M.; Trnka, T. M.; Morgan, J. P.; Grubbs, R. H. *Tetrahedron Lett.* **1999**, 40, 2247.
- (a) Barett, A. *J. Biochem.* **1970**, 117, 601; (b) Liaudet-Coopman, E.; Beaujouin, M.; Derocq, D.; Garcia, M.; Glondi-Lassis, M.; Laurent-Matha, V.; Prebois, C.; Rochefort, H.; Vignon, F. *Cancer Lett.* **2006**, 237, 167.